Role of defects in ferromagnetism in $Zn_{1-x}Co_xO$: A hybrid density-functional study

C. H. Patterson*
Quantum Theory Project, University of Florida, P.O. Box 118435, Gainesville, Florida 32611-8435, USA
(Received 5 December 2005; revised manuscript received 1 September 2006; published 30 October 2006)

Experimental studies of $Zn_{1-x}Co_xO$ as thin films or nanocrystals have found ferromagnetism and Curie temperatures above room temperature and that *p*- or *n*-type doping of $Zn_{1-x}Co_xO$ can change its magnetic state. Bulk $Zn_{1-x}Co_xO$ with a low defect density and x in the range used in experimental thin-film studies exhibits ferromagnetism only at very low temperatures. Therefore defects in thin-film samples or nanocrystals may play an important role in promoting magnetic interactions between Co ions in $Zn_{1-x}Co_xO$. The mechanism of exchange coupling induced by defect states is considered and compared to a model for ferromagnetism in dilute magnetic semiconductors [T. Dietl *et al.*, Science **287**, 1019 (2000)]. The electronic structures of Co substituted for Zn in ZnO, Zn, and O vacancies, substituted N, and interstitial Zn in ZnO were calculated using the B3LYP hybrid density functional in a supercell. The B3LYP functional predicts a band gap of 3.34 eV for bulk ZnO, close to the experimental value of 3.47 eV. Occupied minority-spin Co 3*d* levels are at the top of the valence band and unoccupied levels lie above the conduction-band minimum. Majority-spin Co 3*d* levels hybridize strongly with bulk ZnO states. The neutral O vacancy defect level is predicted to lie deep in the band gap, and interstitial Zn is predicted to be a deep donor. The Zn vacancy is a deep acceptor, and the acceptor level for substituted N is at midgap. The possibility that *p*- or *n*-type dopants promote exchange coupling of Co ions was investigated by computing the total energies of magnetic states of ZnO supercells containing two Co ions and an oxygen vacancy, substituted N, or interstitial Zn in various charge states. The neutral N defect and the singly positively charged O vacancy are the only defects which strongly promote ferromagnetic exchange coupling of Co ions at intermediate range. Total energy calculations on supercells containing two O vacancies and one Zn vacancy clearly show that pairs of singly positively charged O vacancies are unstable with respect to dissociation into neutral and doubly positively charged vacancies; the oxygen vacancy is a "negative *U*" defect. This apparently precludes simple charged O vacancies as a mediator of ferromagnetism in $Zn_{1-x}Co_xO$.

DOI: 10.1103/PhysRevB.74.144432 PACS number(s): 71.20.−b, 71.55.−i, 73.50.−h, 75.70.−i

I. INTRODUCTION

Following initial reports of high-T_c ferromagnetism in $Zn_{1-x}Co_xO$,[1] there have been contradictory reports on the magnetic state of this system.[2–6] Electron paramagnetic resonance (EPR) measurements show that it is possible to produce $Zn_{1-x}Co_xO$ with $x \leqslant 0.1$ (Refs. 7–9) in which Co is substituted for Zn rather than forming clusters. These studies also show that nanocrystalline $Zn_{1-x}Co_xO$ is paramagnetic in this concentration range and at low temperature;[8,9] ferromagnetism was observed only at very low temperature. Another agent must therefore be responsible for promotion of high-T_c ferromagnetism in $Zn_{1-x}Co_xO$. Very recently it has been shown that high-T_c ferromagnetism can be switched reversibly when $Zn_{1-x}Co_xO$ or $Zn_{1-x}Mn_xO$ nanocrystals are capped by O or N (Refs. 6 and 10) or when $Zn_{1-x}Co_xO$ thin films are exposed to Zn vapor.[5] The electric conductivity of ZnO changes markedly when it is annealed in vacuum to produce an *n*-type material,[11,12] while annealing in an oxygen atmosphere restores the insulating behavior of ZnO. Venkatesan *et al.* have shown that the magnetic moment per Co ion in $Zn_{1-x}Co_xO$ at room temperature is reduced from $2.8\mu_B$ per Co ion to zero as the oxygen pressure is varied during annealing.[4]

Here we report results of all-electron B3LYP (Refs. 13 and 14) hybrid density-functional theory (DFT) calculations of the electronic states induced by defects (O vacancy, V_O, Zn vacancy, V_{Zn}, Zn interstitial, Zn_i, and N substituted for O, N_O) as well as the electronic structures of bulk ZnO and $Zn_{1-x}Co_xO$ with $x=0.028$. Several DFT calculations on $Zn_{1-x}Co_xO$ have been reported recently,[15–19] and two of these[16,18] have considered the role of defects in promoting ferromagnetism. One of the difficulties in using DFT to study defects in an insulating material with defect-induced electronic states in midgap is severe underestimation of the band gap and overestimation of exchange coupling constants.[20] In contrast, the B3LYP hybrid functional predicts band gaps for metal oxides which are in good agreement with experimental values[21] and exchange coupling constants which are also in good agreement with experiment.[20] Self-interaction correction of DFT results in an improved prediction for the band gap of ZnO.[18] $Zn_{1-x}Mn_xO$ and $Zn_{1-x}Cu_xO$ have been studied recently using B3LYP hybrid functional calculations.[22]

Defects in ZnO (Ref. 23) and transition-metal-doped ZnO (Refs. 7 and 24–26) were originally studied in the 1960s and 1970s by magnetic resonance and optical techniques. Recent magnetic resonance,[27–32] carrier mobility,[33] positron annihilation spectroscopy,[34] and first-principles calculations[35–37] have given a fuller picture of defect-induced electronic states in ZnO. Magnetic resonance techniques[8,9,38] have been applied to $Zn_{1-x}Co_xO$ and $Zn_{1-x}Mn_xO$ films and nanoclusters. As noted above, these studies[8,9,38,39] as well as x-ray magnetic circular dichroism,[12,39] which probe the local crystal structure about the transition-metal ion, have concluded that the transition-metal ions substitute for a Zn ion. Epitaxial growth of thin films with (110) orientation has been achieved,[12] and there is considerable anisotropy of the magnetism in the thin film.[4]

The remainder of this paper is organized as follows: Details of calculations are described in Sec. II; results of

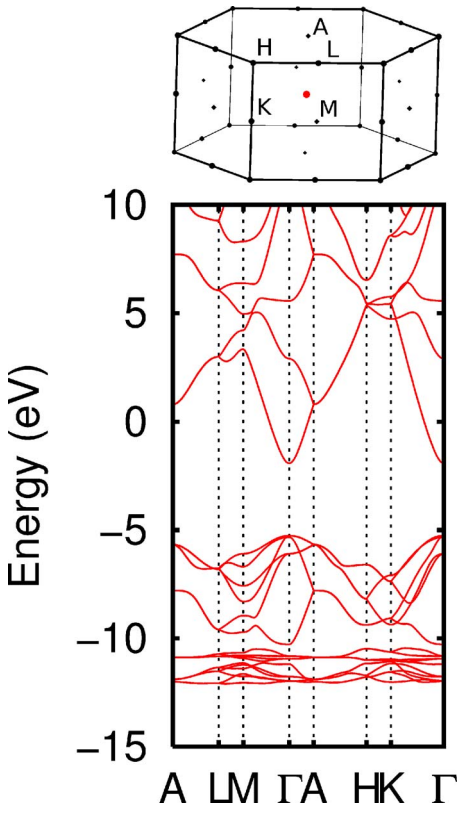

FIG. 1. (Color online) Brillouin zone and band structure for bulk ZnO with the wurtzite structure.

B3LYP calculations on the defects mentioned above, $Zn_{1-x}Co_xO$ as well as two Co ions in the same unit cell as V_O, Zn_i or N_O and two V_O vacancies in the same supercell as a V_{Zn} vacancy, are described in Sec. III; analysis of these results and discussion of the exchange coupling mechanism are given in the final section.

II. DETAILS OF CALCULATIONS

All-electron B3LYP calculations were performed using the CRYSTAL code[40] and a wurtzite structure (space group $P6_3mc$) with fundamental lattice constants 3.249 and 5.206 Å parallel to the a and c axes, respectively.[41] Defect calculations were performed using $3\times3\times2$ supercells with dimensions 9.747 and 10.412 Å parallel to the a and c axes. Thin-film samples of $Zn_{1-x}Co_xO$ which exhibit ferromagnetism are grown on a sapphire substrate[4] which may produce some strain in the samples. The band structure of bulk ZnO was calculated using the wurtzite primitive unit cell and 50 k points in the irreducible Brillouin zone (IBZ), and calculations in the $3\times3\times2$ supercell used 13 k points in the IBZ. The Brillouin zones for the primitive unit cell (Fig. 1) and the supercell have the same symmetry; hence, the same labels are used for high-symmetry points in both cases.

Estimates of the positions of thermodynamic transition levels of the oxygen vacancy were made using the approach described by Van de Walle and Neugebauer.[42] For example, transition levels for charging an acceptor (A) or donor (D) defect are obtained by equating the energy of formation $E^f[X^q]$ of the charged defect (X) (of charge q, with the Fermi level E_F at the acceptor or donor level E_D) to the energy of formation of the neutral defect,

$$E^f[D^+](E_F = E_D) = E^f[D^0]. \tag{1}$$

The formation energy for a charged defect is given by,[42]

$$E^f[X^q] = E_{tot}[X^q] - E_{tot}[\text{bulk}] - n_i\mu_i + q[E_F + E_V + \Delta V], \tag{2}$$

where $E_{tot}[X^q]$ is the total energy of defect X with charge q in a supercell, $E_{tot}[\text{bulk}]$ is the total energy of the bulk solid in the same supercell, and the term $n_i\mu_i$ contains the number n_i of defects and chemical potentials of that species in its native state μ_i. ΔV is a shift in potential required to align the electrostatic potential of the bulk with that of a supercell containing a defect, a "reasonable" distance from the defect.

The final expression for the energy of a donor transition level,[42] in which the Fermi energy is stated with respect to the valence-band maximum (VBM) E_V, is

$$qE_D = E_{tot}[D^0] - E_{tot}[D^+](E_F = 0) - q(E_{corr} + E_V + \Delta V). \tag{3}$$

Differences in total energy in Eq. (3) are estimated using single-particle energy eigenvalues from B3LYP supercell calculations where atomic positions have been relaxed in the presence or absence of a charge on the defect. Where a defect level becomes populated or vacant, the defect energy level relative to the VBM is used to calculate the change in total energy. The energy E_{corr} is a correction energy introduced by Van de Walle and Neugebauer[42] to account for the fact that some single-particle states possess energy minima at symmetry points in the Brillouin zone other than the Γ point. This is not the case for the defects to which this approach is applied here so that E_{corr} is zero. Furthermore, band structure plots of charged and neutral defect states on the same diagram, which have not been shifted in any way, show that there is a negligible shift in the VBM or conduction-band minimum (CBM) position (less than 0.1 eV) so that ΔV is also neglected.

All-electron Gaussian orbital basis sets were used for Zn,[43] O,[44] Co,[45] and N.[46] For vacancy defects, a basis set corresponding to the ion removed was included at the site of the vacancy ion in order to allow a proper description of electrons localized in the vacancy. The local crystal structure around defects was relaxed, and details of their structures are given in the Appendix. In most cases 18 ion positions, including the position of the vacancy site basis set, were relaxed for each defect. These are ions within 3.5 Å of the defect site. Combined crystal structure and spin density plots were generated using the XCrySDen package.[47,48]

III. RESULTS

A. Bulk ZnO

The band structure of bulk ZnO in the wurtzite phase is shown in Fig. 1, and the total bulk density of states is shown in Fig. 2(a). Band energies have not been shifted to align the VBM with any reference energy in order to allow compari-

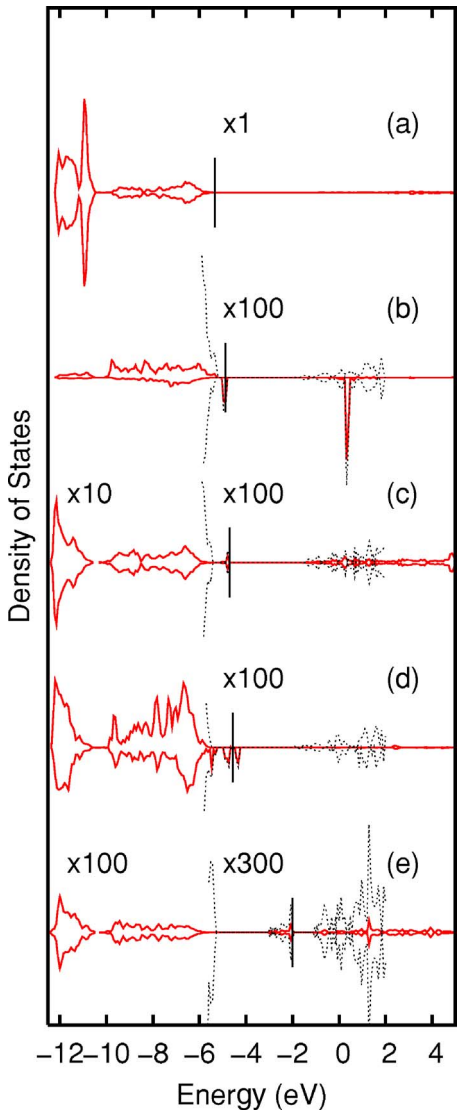

FIG. 2. (Color online) Total and atom-projected densities of states for bulk ZnO and ZnO with various defects from $3\times3\times2$ supercells. Majority-spin densities of states are shown immediately above minority-spin densities of states. The total density of states in the range from −6 to 2 eV is shown to the same scale as the projected density of states in that range as a dotted line. The position of the Fermi energy is shown as a vertical bar. (a) Total density of states for ZnO, (b) projected onto Co atom in Co_{Zn}, (c) projected onto four Zn ions surrounding V_O, (d) projected onto four O ions surrounding V_{Zn}, and (e) projected onto six Zn ions surrounding Zn_i.

son of the band structure when defects are present or absent. The band gap of 3.34 eV obtained using the B3LYP functional is in good agreement with the experimental value of 3.47 eV,[49] and band dispersion in both valence and conduction bands is in good agreement with an earlier plane-wave DFT study[50] and a B3LYP calculation on ZnO.[22] The band gap predicted for ZnO by DFT methods is considerably underestimated, making calculations of positions of defect levels difficult or impossible; DFT pseudopotential calculations predict band gaps of 0.23 eV,[50] 0.91 eV,[51] or 0.81 eV,[35] and the gap depends strongly on the particular pseudopotential used.[50] The B3LYP functional predicts equilibrium a and c lattice constants for wurtzite ZnO which are overestimated by 4% and 1%, respectively.

B. Substituted cobalt Co_{Zn}

Majority- and minority-spin band structures for one Co ion in a $3\times3\times2$ ZnO supercell are shown in Fig. 3, and the Co atom-projected density of states is shown in Fig. 2(b). Occupied *minority*-spin Co $3d$ states with e symmetry are located around 5 eV below the vacuum level, while unoccupied t_2 states are located around the vacuum level. Majority-spin $3d$ states are fully occupied, hybridize strongly with O $2p$ states, and do not appear as a sharp feature in the density of states. By comparing the bulk ZnO band structure with the Co_{Zn} band structure in Fig. 3, it can be seen that there is a minimal change in the ZnO minority-band structure when Co is introduced and that the minority-spin $3d$ states consist of discrete levels. The majority-spin conduction-band structure of Co_{Zn} is nearly identical to that of bulk ZnO, but there is a considerable difference between the majority-spin valence-band structure for ZnO and Co_{Zn}. Results from resonant photoemission experiments[39,52] show a well-defined peak at the top of the valence band as well as a broader density of states due to Co extending down to 8 eV below the Fermi level; the photoemission peak near the Fermi level may therefore arise predominantly from emission from $3d$ minority-spin states. The large energy splitting of occupied e and unoccupied t minority-spin d electrons found here is caused by differences in exchange energies of these levels and not crystal field splitting; a similar study of $Zn_{1-x}Mn_xO$,[22] in which d levels are entirely occupied or entirely empty, shows a crystal field (e and t) splitting of less than 1 eV.

Optical spectra of $Zn_{1-x}Co_xO$ in both earlier single-crystal studies[24,26] and more recent ferromagnetic thin-film studies,[5] show Co^{2+} d-d transitions at midgap in ZnO. However, optical spectra in materials with highly localized excited states yield excitation energies for the N-electron state, but do not provide good estimates of ionization potential and electron affinity differences because the large electron-hole attraction energy in the optically excited N-electron state reduces the excitation energy well below the difference in ionization potential and electron affinity. Photoemission experiments[39,52] and band structure calculations, which involve $N+1$ and $N-1$ electron energy levels, provide the best estimates of the relevant energy level positions. However, observation of photocurrents in $Zn_{1-x}Co_xO$ (Ref. 6) with a subgap conduction threshold may place the unoccupied d levels within the band gap. In order to verify that the single-particle eigenvalues of unoccupied Co $3d$ states with e symmetry for the neutral (N-electron) Zn_{Co} supercell are a reasonable approximation to the electron affinity, a calculation was performed on the supercell with one additional electron. If the single-particle result were unreliable, then one more Co $3d$ state might be populated in a level below the CBM. However, the additional electron is accomodated at the bottom of the conduction band, which shifts to lower energy by 0.4 eV, and the vacant Co $3d$ levels remain empty.

Results for $Zn_{1-x}Co_xO$ presented here may be compared to results of local spin density approximation (LSDA) calcu-

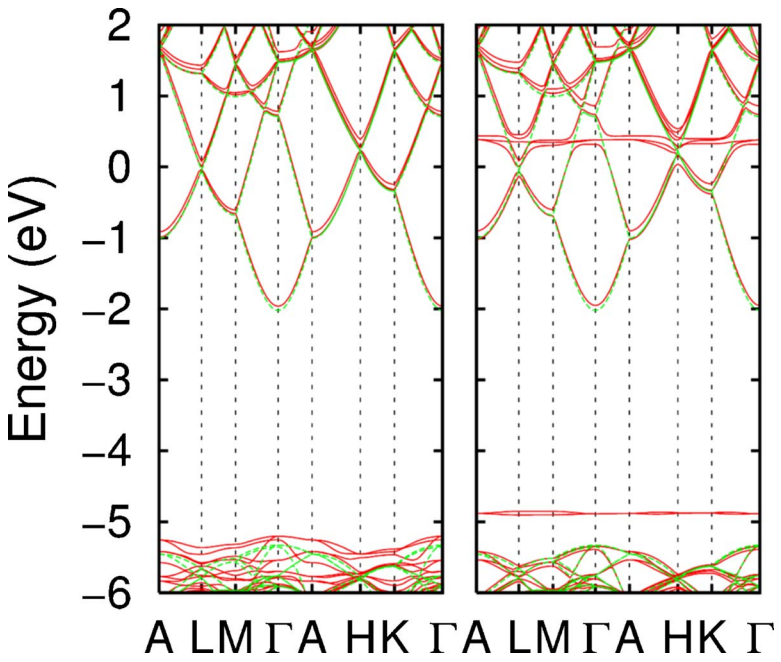

FIG. 3. (Color online) Band structure for Co_{Zn} in a $3\times3\times2$ supercell (solid line) and for bulk ZnO in a $3\times3\times2$ supercell (dotted line). Left panel: majority spin. Right panel: minority spin.

lations by Spaldin.[16] LSDA calculations of the density of states for $Zn_{1-x}Co_xO$ show Co $3d$ levels at the top of the majority-spin valence band. The highest occupied level is a minority-spin $3d$ state approximately 1 eV above the majority-spin $3d$ states. The densities of occupied Co $3d$ states obtained from either B3LYP calculations (this work) or LSDA (Ref. 16) are therefore similar. The main difference in the densities of states occurs in the position of the unnoccupied minority $3d$ states; the B3LYP calculation places these states approximately 5 eV above the minority-spin e states. As explained above, the large splitting of the minority-spin Co $3d$ manifold in the B3LYP calculation is due to the Fock exchange in the B3LYP functional and not the crystal field. Fock exchange in the B3LYP functional also results in an increased band gap of ZnO compared to that predicted by the LSDA. The success of the B3LYP functional in predicting improved properties of metal oxides,[21] compared to DFT or Hartrtee-Fock approaches, may lie in the fact that many-body theories of matter[53] prescribe screening of Fock exchange in solids. Practical experience with the *GW* approximation, starting with a Kohn-Sham Hamiltonian,[54] would suggest that Fock exchange is screened to a large extent; the B3LYP functional contains Fock exchange with a weight factor of 0.2, and this can be regarded as a uniform screening of Fock exchange by 80%.

C. Oxygen vacancy V_O

The neutral oxygen vacancy has two "dangling electrons." B3LYP energy-minimization calculations were performed for one oxygen vacancy in a $3\times3\times2$ supercell in neutral, singly positively charged, and doubly positively charged states. There are major changes in vacancy cavity size and bond distances between Zn ions adjacent to the vacancy and their nearest-neighbor O ions. Bulk Zn-O bond distances are 1.95 Å ($\|c$ axis) and 1.98 Å ($\perp c$ axis); Zn-O bond distances for Zn ions adjacent to the vacancy cavity are 2.00 Å in the neutral vacancy, 1.94 Å in the singly positively charged vacancy, and 1.89 Å in the doubly positively charged vacancy, indicating relaxation of Zn ions into the vacancy for the neutral defect and outward relaxation for the doubly positively charged vacancy. The energy level associated with the two dangling electrons in the neutral vacancy is shown in Fig. 4, and the density of states projected onto the four Zn ions surrounding the vacancy and the vacancy site itself is shown in Fig. 2(c). An inset to Fig. 4 shows positions of energy levels for the charged and neutral defects. The neutral and double positively charged vacancies have spin-zero ground states. The singly positively charged vacancy has a doublet ground state. Positions of donor and acceptor single-particle energy eigenvalues referred to the VBM or CBM of bulk ZnO, respectively, are given in Table I. Transition levels for donor and acceptor states of vacancies studied in this work, obtained using Eq. (3), are given in Table II, where they are compared to values for these levels from the literature.

The neutral, doubly occupied V_O vacancy single-particle level is −3.0 eV below the CBM; when the calculation was repeated with the unit cell singly positively charged, the degenerate vacancy level of the neutral vacancy splits into occupied and unoccupied levels at −2.7 and −1.1 eV (Table I, Fig. 4) in the V_O^+ vacancy. The unoccupied level for the doubly charged vacancy lies 0.6 eV below the CBM. Note that these level positions were determined using defect structures which had been relaxed with the appropriate charge on the defect. (The CRYSTAL program allows charged periodic unit cells to be treated by introducing an effective, compensating uniform background charge.) The fact that the occupied level of the V_O^+ vacancy is higher in energy than the occupied level of the neutral V_O vacancy indicates that this is a "negative-U" defect, as the positively charged ion is more readily ionized than the neutral defect. The same conclusion regarding the nature of the V_O defect can be drawn from the fact that the electron affinity level for the V_O^{2+} vacancy is higher in energy than the V_O^+ vacancy (Fig. 4, inset). The

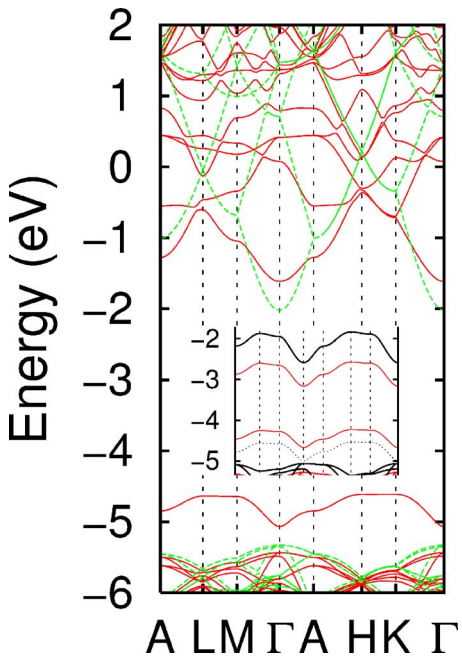

FIG. 4. (Color online) Band structure for V_O in a $3\times3\times2$ supercell (solid line) and for bulk ZnO in a $3\times3\times2$ supercell (dotted line). The single-particle energy eigenvalue for the neutral V_O vacancy is located around 5 eV below the vacuum level. The inset shows how this level changes when the charge and structure of the vacancy change. In order of increasing energy the levels are occupied state V_O^0, and occupied state V_O^+, unoccupied state V_O^+, and unnoccupied state V_O^{2+}.

negative-U character of the defect is also indicated by the position of the $\epsilon(2+|0)$ transition level (−3.0 eV), which lies below the $\epsilon(2+|+)$ level (−2.7 eV). There is considerable dispersion of the defect levels because tails of wave functions associated with the defect extend beyond supercell boundaries. Previous DFT calculations[51,56] on this defect have shown that the defect level wave function has large amplitude on the shell of O ions outside the shell of Zn ions closest to the vacancy site.

TABLE I. Positions and occupations of single-particle defect levels in eV at the Γ point of the IBZ referred to the conduction-band minimum (donors) or valence-band maximum (acceptors) of bulk ZnO.

Donor charge state	V_O	Zn_i
Neutral	−3.0	−0.9
1+ (occupied)	−2.7	−1.2
1+ (vacant)	−1.2	−0.3
2+ (vacant)	−0.6	
Acceptor charge state	V_{Zn}	N_O
Neutral (occupied)	0.8	0.3,1.2
Neutral (vacant)	0.9,0.9	1.2
1− (occupied)	0.4,0.5	0.8,1.0,1.0
1− (vacant)	1.0	
2− (occupied)	0.7,0.8,0.8	

In order for magnetic oxygen vacancies to exist in ZnO, there must be a sink for electrons and the charged vacancies created must remain singly charged. If V_O is a negative-U defect, as has been suggested previously,[36,51] two singly charged vacancies will spontaneously disproportionate to a neutral and a doubly charged vacancy. A B3LYP total energy calculation was performed with one V_{Zn} and two V_O defects in an uncharged $3\times3\times2$ supercell in order to test the possiblity of forming V_O^+ defects in ZnO. Positions of ions surrounding each vacancy were relaxed as in other supercell calculations.

Energy minimization calculations were performed with a total spin of 1 or 0 (i.e., $2\mu_B$ or $0\mu_B$) per unit cell. A state with a single positive charge on each V_O should be well described by a wave function with total spin 1; the fact that the spins are parallel ensures that one electron is located on each site. A state with a double charge on one vacancy and no charge on the other should be well described by a wave function with total spin 0 as the electrons are properly described as a pair in a single orbital on one vacancy site. The wave function from the calculation with total spin 1 has spin density localized on both V_O sites and the V_{Zn} site, demonstrating that two V_O vacancies were formed which could be described as "singly charged" spin-half. The total magnetic moment associated with each V_O and four surrounding Zn ions was $0.55\mu_B$; that associated with V_{Zn} and four surrounding O ions was also $0.55\mu_B$, and the remaining $0.35\mu_B$ was distributed over the remainder of the supercell.

The energy-minimzed structure with spin 1 had fairly similar bond lengths in either V_O vacancy and average Zn-O bond lengths for Zn ions lying on the vacancy boundary of 1.93 Å and 1.94 Å, indicating roughly equivalent vacancies. On the other hand, the energy-minimized structure with spin 0 had distinctly different bond lengths in either V_O vacancy and average Zn-O bond lengths for Zn ions on each vacancy boundary of 1.88 and 2.01 Å (cf. 1.89 and 2.00 Å found for single vacancies in these two charge states), indicating two distinct vacancy types. The energy of the structure with spin 0 (i.e., charge disproportionated) was lower than that for the energy-minimized structure with spin 1 (i.e., no charge disproportionation) by 1.4 eV; this energy difference may be compared to a value of 1.3 eV obtained by Zhang and co-workers.[36] These results indicate that the V_O^+ defect is indeed a negative-U defect and spontaneously dissociates into V_O and V_O^{2+}.

D. Zn vacancy V_{Zn}

Zn vacancies are believed to be the dominant deep acceptor states in ZnO.[34,57] All of the charge states of defects discussed so far, with the exception of the singly positively charged V_O state, have closed-shell ground states and no unpaired electrons. The neutral Zn vacancy contains two "dangling holes" so that the minority-spin band structure consists of two singly occupied bands and two empty bands (Fig. 5). These mainly consist of four O $2p$ orbitals on the O ions which surround the vacancy site, and they form nondegenerate and quasi-triply-degenerate states with a and t point symmetries. In the neutral V_{Zn} defect the a state lies just above

TABLE II. Transition levels (TL) and single-particle eigenvalues (SP) for defects in bulk ZnO in eV. Donors are referred to the conduction-band minimum of bulk ZnO and acceptors to the valence-band maximum.

V_O	B3LYP TL (this work)	B3LYP SP	LDA TL[a]	LDA+U TL[a]	LDA+U TL (extrap.)[b]
$\epsilon(+\|0)$	−3.3	−3.0	−2.4	−0.9	−1.5
$\epsilon(2+\|+)$	−2.7	−1.2	1.2	+0.2	−0.5
$\epsilon(2+\|0)$	−3.0	−0.6	−0.6	−0.3	−1.0
Zn_i					
$\epsilon(+\|0)$	−0.6	−0.9	0.8		
V_{Zn}					
$\epsilon(0\|-)$	0.0(3)	0.9	−0.5		
$\epsilon(-\|2-)$	0.8	1.0	0.0		
$\epsilon(0\|2-)$	1.5	0.9	−0.3		
N_O					
$\epsilon(0\|-)$	1.4	1.2			

[a]Reference 36.
[b]Reference 55.

the VBM and the t state lies above that. The degeneracy of the t state is broken to allow occupation of one of these orbitals. Breaking of the t degeneracy ought to lead to a Jahn-Teller distortion of the tetrahedra of O ions surrounding the vacancy, but there was little symmetry breaking when two shells of ions surrounding the vacancy were relaxed. The two electrons in singly occupied orbitals exist either as a spin singlet ($S=0$) or triplet ($S=1$). The wave function form used in most band theories (including the form used here) consists of single determinants for up and down spins and can only describe the spin-triplet state of the vacancy. It is therefore not possible to predict whether the neutral V_{Zn} vacancy will have a nonmagnetic, singlet or magnetic, triplet ground state on the basis of these calculations.

Single-particle energy eigenvalues and transition levels for the V_{Zn} vacancy are given in Tables I and II, respectively. The B3LYP supercell calculation places the $\epsilon(+|0)$ transition level just above the VBM (by 0.03 eV) and the transition level to add a further electron, $\epsilon(-|2-)$, at +0.8 eV. The $\epsilon(0|2-)$ level is located at higher energy, 1.5 eV, indicating that the V_{Zn}^{-} defect is stable. Similar trends are found for transition levels calculated using the LDA,[36] except that these levels lie below the VBM and will be occupied even with the Fermi level at the VBM.

E. Zn interstitial Zn_i

Shallow donor states estimated to lie 30 meV below the ZnO CBM have been observed in ZnO subjected to electron irradiation and have been assigned to Zn_i or Zn_i complexes.[33] The energetically favorable site for a single Zn interstitial in ZnO is the octahedral site.[51] The band structure for a 3×3

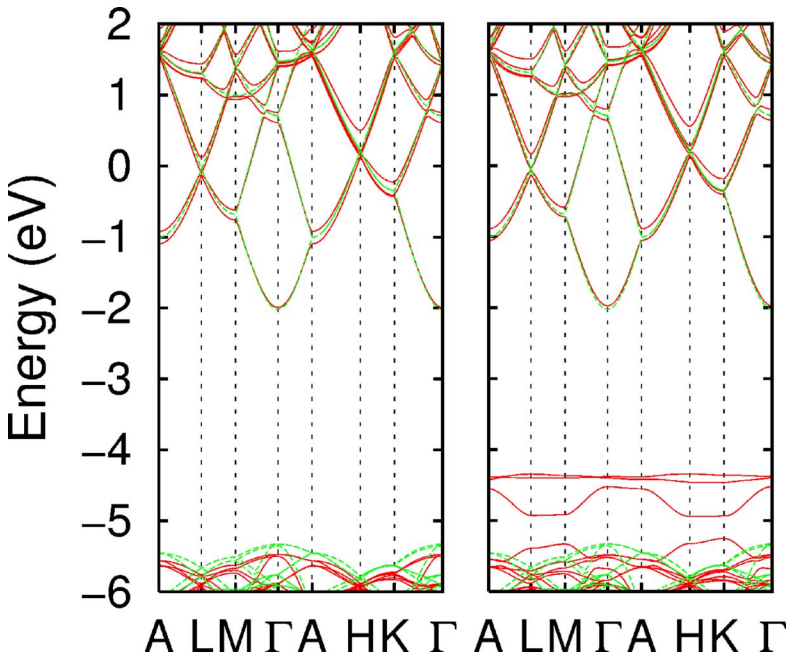

FIG. 5. (Color online) Band structure for V_{Zn} in a $3\times3\times2$ supercell (solid line) and for bulk ZnO in a $3\times3\times2$ supercell (dotted line). Left panel: majority spin. Right panel: minority spin.

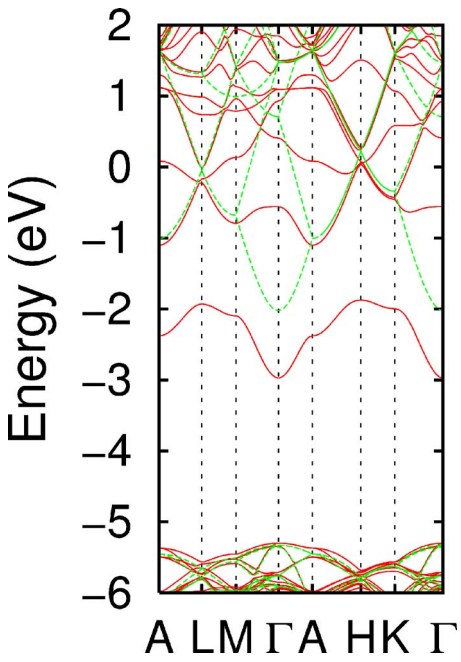

FIG. 6. (Color online) Band structure for Zn_i in a $3\times3\times2$ supercell (solid line) and for bulk ZnO in a $3\times3\times2$ supercell (dotted line).

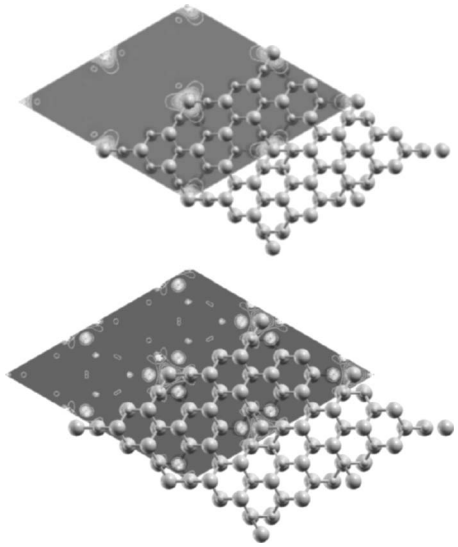

FIG. 7. Spin density for Zn_i in a $3\times3\times2$ supercell with unit positive charge. Upper panel: spin density in a plane containing interstitial Zn ions. Lower panel: spin density in a plane perpendicular to the *c* axis containing Zn ions closest to interstitial ions. O ions are indicated by small gray spheres and Zn ions by large gray spheres.

$\times2$ ZnO supercell with a single Zn interstitial at the energy-minimzed octahedral site is shown in Fig. 6. A new defect level is formed after hybridization of the 4*s* level of the Zn interstitial and the lowest conduction band (which is predominantly of Zn 4*s* character). The density of states for the Zn interstitial and the six Zn ions nearest to it is shown in Fig. 2(e). The atom-projected density-of-states plot shows that the defect level lies just below the CBM of bulk ZnO (shown in Fig. 6 as a dotted line with a minimum energy of −2.0 eV). The defect level disperses by about 1 eV throughout the Brillouin zone, and the conduction band is considerably modified at low energies. This level is likely to arise in the following way: the 4*s* level of the Zn atom *in vacuo* must lie close to the bottom of the bulk conduction band, which is derived principally from bulk Zn 4*s* states. There is therefore strong interaction between the localized interstitial Zn 4*s* level and the conduction band, and an avoided crossing of levels results in the splitting-off of the bottom of the conduction band with a large admixture of the interstital ion 4*s* state. In a larger supercell with much reduced defect interactions, this strongly dispersive level would likely consist of a sharper level within a few tens of meV of the CBM [the density-of-states plot in Fig. 2(e) shows that the density of states for this level lies just below the bulk CBM], which would confirm the assignment of the state observed in experiment.[33]

The transition level and single-particle energy eigenvalues for the $\epsilon(0|+)$ transition are given in Table II. The single-particle eigenvalue is −0.9 eV below the CBM at the Γ point, and the transition level is at −0.6 eV below the CBM.

Zn_i in a positive-ion state has been proposed as a possible mediator of ferromagnetism in $Zn_{1-x}Co_xO$.[5] In order to be effective as a mediator of ferromagnetism, the spin density of the defect ought to overlap the pair of transition-metal ions to a significant degree. Visualization of the spin density as a contour plot superposed on the defect and bulk crystal structures can provide information on the degree of overlap of the spin density of a defect with a transition-metal ion. The spin density for Zn_i in a $3\times3\times2$ supercell with one electron removed per unit cell is shown in Fig. 7. The plot shows that the spin density for the positive-ion state is localized chiefly on the interstitial ions plus the 12 Zn and O ions surrounding it; this was also found to be the case for the charge density for the neutral interstitial associated with the defect level just below the CBM. The magnetic moment on the interstitial Zn_i^+ ion determined by a Mulliken population analysis is $0.37\mu_B$, and the moments on the six Zn and six O ions immediately surrounding the vacancy are $0.049\mu_B$ (Zn $\times3$), $0.027\mu_B$ (Zn $\times3$), $0.018\mu_B$ (O $\times3$), and $0.013\mu_B$ (O $\times3$), giving a net moment of $0.69\mu_B$ on the 13-ion Zn_i complex and $0.31\mu_B$ on the remaining ions in the supercell.

F. Substituted nitrogen N_O

Recently it has been shown that N doping can be used to produce *p*-type ZnO,[58] and there have been several theoretical studies of codoped N in $Zn_{1-x}Co_xO$ and $Zn_{1-x}Mn_xO$.[18,59] Nitrogen forms a substitutional defect in ZnO,[28] where it leads to introduction of a hole. Symmetry constraints allow the hole to be mainly associated with a nearly degenerate pair of N 2*p* orbitals lying in the *ab* plane of the wurtzite structure *or* in a nondegenerate 2*p* orbital parallel to the *c* axis. The former orbital occupation was found in the geometry optimized structure for N_O and the semimetallic band structure is shown in Fig. 8, where the partially occupied, weakly dispersive and fully occupied, nondegenerate N 2*p* states lie above the ZnO occupied states.

The density of states for the neutral ZnO supercell with one N_O substitution is shown in Fig. 9(b); the single-particle

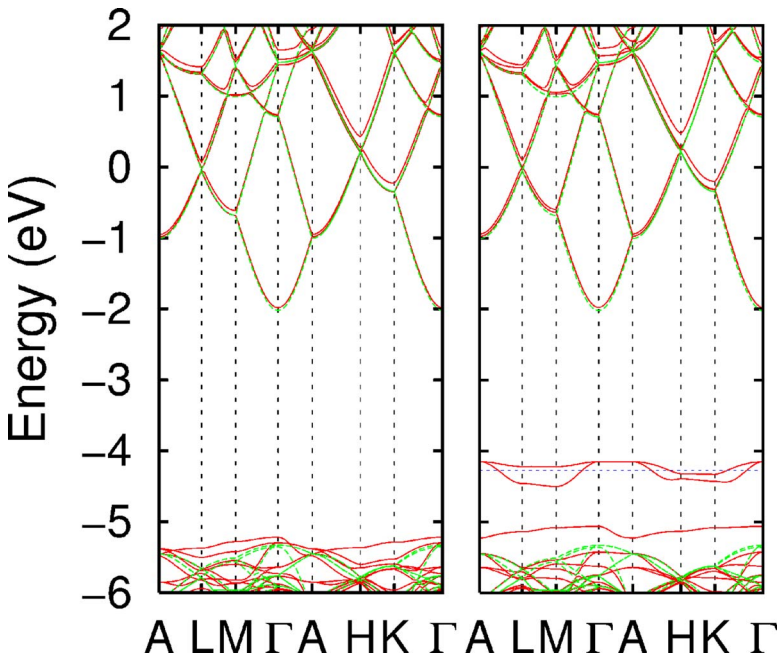

FIG. 8. (Color online) Band structure for N_O in a $3\times3\times2$ supercell (solid line) and for bulk ZnO in a $3\times3\times2$ supercell (dotted line). Left panel: majority spin. Right panel: minority spin. The position of the Fermi level is shown as a horizontal dotted line in the minority-spin band structure.

energy eigenvalue for the $\epsilon(0|-)$ acceptor level is 1.2 eV above the VBM (Table II), in good agreement with the transition level (1.4 eV above the VBM).

A plot of the spin density for the neutral N_O-substituted supercell is shown in Fig. 10. The spin density from the N ion delocalizes onto nearby O ions in the same plane (perpendicular to the c axis), and nearly all spin density is confined to this plane. The magnetic moment on each N ion is $0.66\mu_B$, and on the O ions with the largest moments, it is $0.03\mu_B$.

G. Substituted cobalt with V_O^{n+}, N_O, or Zn_i^{n+}

The possibility that neutral or positively charged defects can mediate ferromagnetic interactions in ZnO at intermediate range (i.e., just beyond near-neighbor distances) with a strength that could result in Curie temperatures in $Zn_{1-x}Co_xO$ above room temperature was investigated using total energy calculations. A defect which mediates ferromagnetism will most likely be magnetic itself as induced magnetic polarization of the defect is unlikely to result in strong mediation of ferromagnetism. Total energy calculations were performed with two Co ions and one defect per $3\times3\times2$ unit cell and the magnetic moments of the Co ions parallel or antiparallel. The minimum distance between Co ions in the lattice was 7.66 Å, and the Co-V_O and Co-N_O minimum distances were 4.94 and 5.00 Å. The same Zn sites were substituted for Co in Co/V_O, Co/N_O, and Co/Zn_i calculations. The same O sites were substituted by V_O or N, allowing a direct comparison of the efficacy of magnetic coupling of these defects in various charge states. In Co/Zn_i calculations the minimum Co-Zn_i distances were 5.10 and 6.68 Å. The total energy difference between the two magnetic states for two Co ions in a $3\times3\times2$ supercell in the absence of a defect is less than 1 meV.

When a N_O defect was introduced, the ferromagnetic configuration of the Co ions was 27 meV lower in energy than the antiferromagnetic configuration. Densities of states for the N_O ion and the N_O ion plus two Co ions per supercell are compared in Figs. 9(b)–9(d). When Co is present in the unit cell, states around the Fermi energy are mainly of Mn $3d$ e character. The empty minority-spin level mainly localized on the N ion is located 1.4 eV below the CBM.

When a V_O vacancy was introduced, total energy differences for the two magnetic states were less than 1 meV for either V_O or V_O^{2+} and 36 meV for a V_O^{+} vacancy (with the ferromagnetic state of the Co ions lower in energy). The spin density for two Co ions and a V_O^{+} vacancy with the Co majority spins parallel to each other is shown in Fig. 11, and the density of states projected onto the two Co ions is shown in Fig. 9(e).

Density-of-states plots for either V_O or N_O combined with two Co in a unit cell are quite similar, and it is not surprising that the energy differences between ferro and antiferromagnetic configurations of the Co ions in the presence of these defects are also quite similar. In either case the empty state associated with the vacancy can be seen in the majority-spin density around −3 eV.

When a Zn_i interstitial was introduced, the total energy difference was less than 1 meV for either the neutral or singly positively charged states of the defect.

IV. DISCUSSION

A. Single defects

Recent positron annihilation experiments[32] found that the V_O defect in ZnO subjected to irradiation by high-energy electrons is neutral at low temperature and is 10 times more abundant than the V_{Zn} vacancy. Thermodynamic arguments,[36,51,60] which take energy levels from DFT calculations corrected for the band-gap error, have shown that V_O is the most thermodynamically stable defect under Zn-rich conditions. The positions of the $\epsilon(0|+)$ level of V_O are predicted

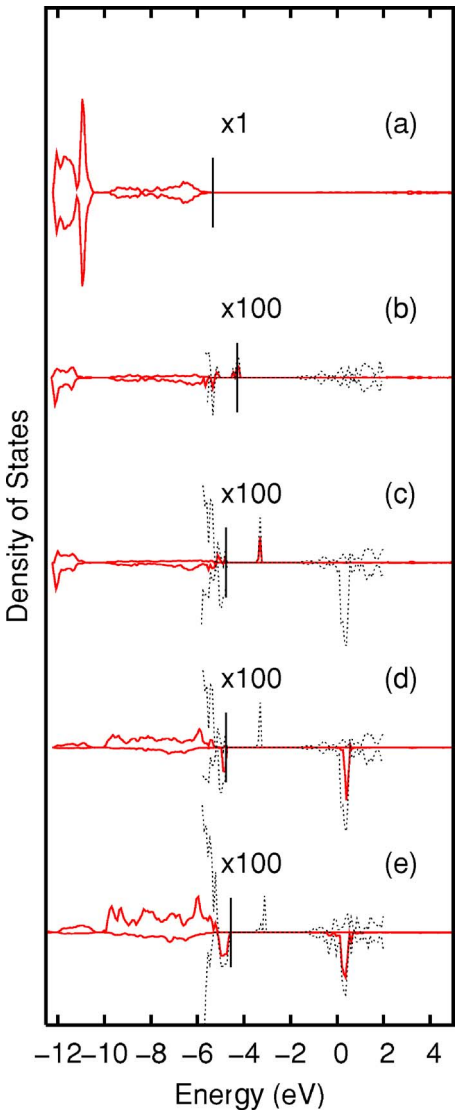

FIG. 9. (Color online) Total and atom-projected densities of states for bulk ZnO and ZnO with various defects combined with Co ions from $3\times3\times2$ supercells. Majority-spin densities of states are shown immediately above minority-spin densities of states [with the exception of (b) where the order is inverted]. The total density of states in the range from −6 to 2 eV is shown to the same scale as the projected density of states in that range, as a dotted line. The position of the Fermi energy is shown as a vertical bar. (a) Total density of states for ZnO, (b) projected onto N ion in N_O, (c) projected onto N ion in N_O with two Co ions per unit cell, (d) projected onto two Co ions in N_O with two Co ions per unit cell, and (e) projected onto two Co ions in V_O with two Co ions per unit cell. Scaling factors which have been used are indicated.

to be 1.0,[55] 2.4,[36] or 3.3 eV (this work) below the CBM; a nonlinear spectroscopy study[61] found this level to lie 2.1 eV below the CBM.

The position of this level has been inferred from 600-nm photoluminescence (PL) observed in native ZnO by optical detection of electron paramagnetic resonance (ODEPR).[31] The process which has been proposed[31] to account for the observed PL is a transition in which a neutral

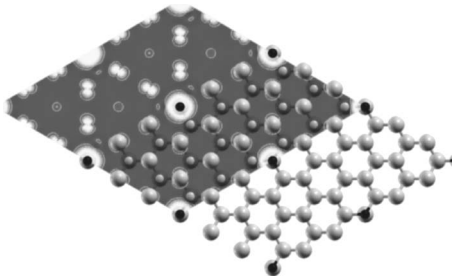

FIG. 10. Spin density for N_O in a $3\times3\times2$ supercell in a plane perpendicular to the c axis containing only N and O ions. O and N ions are indicated by small gray and black spheres, respectively, and Zn ions by large gray spheres.

effective mass donor EM^0 transfers an electron to a singly positively charged oxygen vacancy,

$$EM^0 + V_O{}^+ \rightarrow EM^+ + V_O{}^0. \quad (4)$$

The singly charged $V_O{}^+$ state is invoked as the process is observed to be spin dependent; the metastable $V_O{}^+$ state is believed to be formed by optical illumination in the ODEPR experiment.[31] One model for the PL (Ref. 31) is that the effective mass donor level lies close to the CBM and the transition observed in PL is transfer of an electron to the $\epsilon(0|+)$ level, which, given the PL wavelength, would lie up to 1 eV above the VBM. The alternative model[31] is that the $\epsilon(0|+)$ level lies up to 1 eV below the CBM and that the observed PL arises from hole capture by the V_O vacancy. In the former model, the transition involving the V_O vacancy is directly observed in the experiment, while in the latter it is only indirectly observed. The $\epsilon(0|+)$ level is predicted to lie deep in the band gap (Table II) by LDA (Refs. 36 and 55) or B3LYP calculations (this work), and therefore support a model in which the V_O defect is the lower level in the transition. However, the $\epsilon(0|+)$ level is shifted up in the band gap in an LDA+U calculation[55] and this calculation supports a model in which the V_O defect is the upper level in the transition.

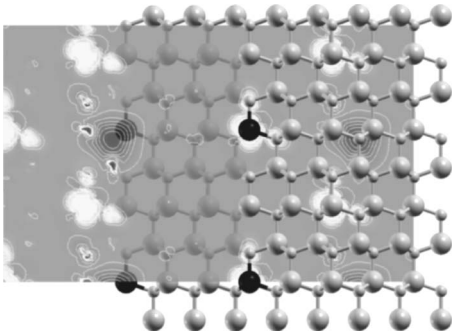

FIG. 11. Spin density for two Co ions and a $V_O{}^+$ defect in a $3\times3\times2$ supercell. O ions are indicated by small gray spheres, and Zn and Co ions are indicated by large gray and black spheres, respectively. Spin density on the defect appears as a roughly spherical density while spin density on Co ions has a mixed-d and tetrahedral-lobe character.

Using thermodynamic arguments, Kohan and co-workers,[51] Zhang and co-workers,[36] Janotti and van de Walle,[55] and the present author (this work) have found that the V_O defect is a negative-U defect. The value of U is the difference, $\epsilon(+|0)-\epsilon(2+|+)$, since this equals the difference in formation energies $E^f[V_O{}^{2+}+E^f(V_O{}^0)-2E^f(V_O{}^+)]$. Predicted values for U are, therefore, −3.6 eV (Ref. 36) (the authors of that paper quote a value of −0.6 eV without LDA gap correction), −1.0 eV (Ref. 55), and −0.6 eV (this work). The $\epsilon(2+|0)$ transition level is found at −0.6 eV,[36] −1.0 eV,[55] or at −3.0 eV (this work). The calculation described above, in which two V_O and one V_{Zn} vacancies were placed in the same $3\times3\times2$ supercell, as well as the relative ordering of $\epsilon(+|0)$, $\epsilon(2+|+)$, and $\epsilon(2+|0)$, confirm that V_O is a negative-U defect, so it is unlikely that isolated V_O defects are the main mediators of ferromagnetism in $Zn_{1-x}Co_xO$.

Positron annihilation studies of electron-irradiated ZnO (Refs. 32 and 34) have shown that V_{Zn} vacancies exist in a negatively charged state and have given an estimate for the ionization energy of V_{Zn} vacancies of 2.3 eV.[32] The $\epsilon(-|2-)$ transition level is 0.8 eV above the VBM (or 2.5 eV below the CBM) (Table II), in reasonable agreement with this value.

The Zn_i interstitial is known to be a shallow donor and estimates[27,33,61–63] of the position of the donor level range between 30 meV (Ref. 33) and 200 meV (Ref. 61) below the CBM. DFT studies,[36,51] where corrections have been made for the band-gap error, find that this level lies above the CBM so that Zn_i is spontaneously doubly ionized. The B3LYP calculations presented here show that the Zn 4s level in Zn_i hybridizes strongly with the ZnO conduction band and forms a strongly dispersive band which lies just below the CBM. The $\epsilon(+|0)$ transition level is −0.6 eV below the CBM. This value was calculated using the single-particle energy eigenvalue at the Γ point of the IBZ in Eq. (3); there is considerable dispersion of this level which has its lowest energy at the Γ point. A calculation on a larger supercell (say, $5\times5\times3$) would yield a state with less dispersion and a value for the transition energy closer to the range of experimental values.

B3LYP calculations for N_O presented in Fig. 8 show a semimetallic electronic structure for this defect with the Fermi level 1.2 eV above the VBM. The $\epsilon(0|-)$ transition level for this defect is 1.4 eV above the VBM. An earlier DFT study of this system found the acceptor level for N_O to be 0.4 eV above the VBM.[37] In optical PL experiments the acceptor level in p-type ZnO implanted with N was found to be in the range 0.17 to 0.20 eV,[64] well below the value found in the B3LYP calculations. In a self-interaction corrected (SIC) LSDA study of the $Zn_{1-x}Co_xO$ system with one Co and one N per unit cell, the ground-state configuration of the Co ion was found to be Co^{3+}; i.e., there is an electron transfer from the Co ion to the N defect. This electron transfer is not found in the present B3LYP calculations, where the Co ion remains in a 2+ state. The result that N_O promotes ferromagnetism in $Zn_{1-x}Co_xO$ differs from the experimental finding that N capping of $Zn_{1-x}Co_xO$ nanocrystals containing 3.5% Co results in paramagnetic nanocrystals while O capping of these nanocrystals results in weak ferromagnetism.[6]

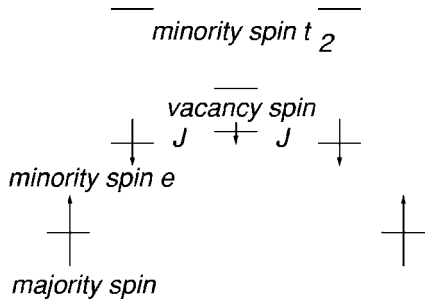

FIG. 12. Single-particle orbital diagram for two Co ions and a $V_O{}^+$ oxygen vacancy in the ferromagnetic ground state. The exchange integrals which are important for ferromagnetic exchange coupling are shown as J symbols. The empty orbital above the vacancy spin label is the one vacated when the defect is ionized. This is not the many-particle acceptor state in which the bound vacancy spin becomes a free carrier.

B. Exchange coupling mechanism

A mechanism of exchange coupling has been proposed by Dietl *et al.*[65] to account for ferromagnetism in zinc-blende semiconductors, particularly $Ga_{1-x}Mn_xAs$; Mn^{2+} $3d^5$ ions substitute for Ga^{3+} ions and so introduce a shallow acceptor state with a binding energy of order 100 meV.[65] The key elements of this mechanism are an unpaired electron in the valence band whose wave function overlaps that of the transition-metal ion and whose spin is *opposite* to that of the transition-metal ion. In the particular case of $Ga_{1-x}Mn_xAs$, a 2+ ion is substituted for a 3+ ion, so that the substitution simultaneously produces a transition-metal ion magnetic moment and an unpaired electron state with appropriate spin. On the other hand, when Co is substituted for Zn, a transition-metal magnetic moment is introduced, but since Co^{2+} and Zn^{2+} are isovalent, no unpaired electron is available to produce exchange coupling. Introducing a defect with a spin, such as $V_O{}^+$ or N_O, provides the magnetic state necessary for exchange coupling and as long as the defect is not too distant from the transition metal, a substantial wave function overlap is attainable between the electron associated with the magnetic defect and the transition-metal ion. A plausible mechanism for the energy lowering, when the transition-metal ion spins are parallel rather than antiparallel, is that the unpaired electron may be delocalized into both sets of empty transition-metal d states only when their total spins are parallel. The arrangement of single-particle states and spins for a $V_O{}^+$ defect coupling two Co^{2+} ions is shown schematically in Fig. 12. Some evidence for this type of mechanism may be found by inspecting Mulliken spin populations from B3LYP calculations for either relative orientation of the Co magnetic moments. Mulliken spin and charge populations for two Co ions in the presence of a $V_O{}^+$ vacancy in either ferromagnetic or antiferromagnetic configurations show that when the Co spins are parallel, the spin localized on the $V_O{}^+$ vacancy decreases by around $0.1\mu_B$ compared to when the spins are antiparallel. Since this is an insulating state, the total magnetic moment in the supercell remains constant. This shows that there is greater delocalization of the vacancy spin and consequently greater overlap with the region where empty Co d levels are located when Co spins are *parallel*.

The mechanism for exchange coupling in a range of dilute magnetic semiconductors (DMS's) has been discussed by Sato and Katayama-Yoshida. Using a DFT coherent potential approximation[59] they studied a wide range of transition-metal-doped II-VI and III-V semconductors. They find a ferromagnetic ground state for $Zn_{1-x}Co_xO$ with an onset of ferromagnetism around 10% Co concentration, which is higher than the 2.8% Co concentrations used in this work. They postulate that stabilization of ferromagnetism is due to a double-exchange mechanism and that this is most efficient when there is partial occupation of minority-spin transition-metal 3*d t* states.[59]

Substantial ferromagnetic exchange coupling was found only in two instances in this work, and both involve a defect with a magnetic moment and defect spin densities which overlap with Co-ion spin densities. The ground-state configuration is one where majority Co *t* spins are parallel and minority *e* spins are parallel to each other and the vacancy spin (Fig. 12). Direct exchange coupling of Co ions at the separation used for this study is less than 1 meV, as demonstrated by total energy calculations when no oxygen vacancy is present. When a defect with a spin is present (N_O or V_O^+), a total energy difference of the order of 30 meV is found, but when when the spin on the V_O^+ vacancy is removed by further ionization of the vacancy, the total energy difference of parallel and antiparallel spin configurations is reduced from 36 to 1 meV, demonstrating the importance of the spin of the defect in promoting ferromagnetic exchange coupling.

Experiment[4] shows that ferromagnetism of $Zn_{1-x}Co_xO$ in *n*-type ZnO is destroyed by annealing in oxygen. Spinless V_O and V_O^{2+} defects do not provide the necessary magnetic coupling of transition-metal ions; since there is evidence that V_O^+ spontaneously disproportionates into these spinless vacancies from several theoretical studies,[36,51] including this work, it seems unlikely that simple O vacancies are the promoters of ferromagnetism in $Zn_{1-x}Co_xO$ unless magnetic V_O^+ or similar defects are stabilized by some mechanism. Recent valence-band x-ray photoelectron spectra of $Zn_{1-x}Co_xO$ samples which have been prepared under conditions which result in ferromagnetic thin films (600 °C substrate temperature during deposition) or nonmagnetic (450 °C) (Ref. 66) show very different photoelectron spectra in the region above O 2*p* emission; spectra from nonmagnetic samples show a peak around 1 eV above the top of the O 2*p* band which may be due to emission from Co 3*d e* states while ferromagnetic samples show photoemission in two broad peaks just above the top of the O 2*p* band extending to 2 eV into the band gap. This additional photoemission in ferromagnetic samples must be due to defect states, and the photoelectron cross section is more than 5% of the total O 2*p* cross section, indicating a very high defect density. Under these circumstances it is possible that magnetic defects do exist which promote the ferromagnetism.

No substantial exchange coupling was found for either the neutral or positively charged Zn_i^+ defect, contrary to the finding that exposure of samples to Zn vapor results in promotion of ferromagnetic exchange coupling;[6] the latter defect is spin $\frac{1}{2}$ and might therefore be expected to result in exchange coupling of Co ions. The absence of exchange coupling may be because the spin associated with the interstitial Zn ion does not overlap the Co ion wave function either spatially or energetically in the configuration studied.

An alternative possibility for the agent which promotes exchange coupling in $Zn_{1-x}Co_xO$ is atomic hydrogen. In an LDA study,[67] Park and Chadi showed that hydrogen in an interstitial site adjacent to two Co ions in $Zn_{1-x}Co_xO$ strongly promoted exchange coupling of the Co ions. A B3LYP calculation was performed for one H atom and two Co ions in a $3\times3\times2$ ZnO supercell. The H atom was bond centered in a ZnO bond approximately 5 Å from the Co ions, and the Co ions were in the positions used for other exchange coupling calculations in the $3\times3\times2$ supercell. After geometry relaxation the H atom defect resulted in a nonmagnetic metallic state and there was no promotion of exchange coupling in this atomic configuration. Note that the atomic configurations used in the LDA study[67] and in this work are very different; in the former study the H atom is a nearest neighbor of two Co ions whereas in the latter they are much further separated and this may explain the difference in results obtained.

The exchange coupling mechanism outlined here is essentially the same as the impurity-band model of Coey *et al.*[68] in which there is strong spatial and energetic overlap between an impurity band associated with a defect and a filled *d* band. A double-exchange mechanism of ferromagnetic coupling in $Zn_{1-x}Co_xO$ and $Zn_{1-x}Mn_xO$ has been outlined, for example by Petit *et al.*[18] or Kittilstved *et al.*,[6,69] in which certain charge fluctuations are only permitted for the ferromagnetic state. These charge fluctuations generally lower the total energy, and changes to the energy and wave function can be estimated using perturbation theory. In the approach used here, energy differences and changes to the wave function are obtained in the self-consistent field calculation.

C. Summary

The electronic structures of wurtzite ZnO with Co substituted for Zn, oxygen, and zinc vacancies, a zinc interstitial, and nitrogen substituted for oxygen have been computed using the B3LYP hybrid density functional in $3\times3\times2$ supercells. The B3LYP hybrid density functional used in this work differs from other density functionals in that it contains exact exchange (with a weight of 20% of the full exact exchange in Hartree-Fock theory). The band gap of oxides predicted by B3LYP and similar functionals, where just the weight of exact exchange is varied,[21] depends strongly on this weight, and an argument for the success of B3LYP in predicting band gaps of oxides can be made in terms of screening of exact exchange in the *GW* approximation. The use of the B3LYP functional for predicting positions of transition levels of defects in oxides needs to be studied further. The $\epsilon(0|+)$ donor level for the Zn_i interstitial in ZnO is found to be 0.6 eV below the CBM whereas it is found to lie 30 meV below the CBM in experiment. The N acceptor level in N-doped ZnO is predicted to be 1.2 eV above the VBM while it is found to be around 0.2 eV above the VBM in a PL experiment. Total

energy calculations have been performed for two Co ions in a $3\times3\times2$ supercell with an oxygen vacancy, zinc interstitial, and substituted nitrogen. Neutral and positively charged states of the oxygen vacancy and zinc interstitial were studied. Only the singly positively charged oxygen vacancy and neutral substituted N defects resulted in a substantial exchange coupling of two Co ions at intermediate range (>7 Å). Total energy calculations were performed with two oxygen vacancies and one Zn vacancy in a neutral supercell. A state with two distinct O vacancy cavities, characteristic of charge disproportionation of the vacancies into a neutral and doubly charged vacancy, was substantially lower in energy than one with similar cavities, characteristic of two equivalent singly charged vacancies. Disproportionation of magnetic, singly charged vacancies into nonmagnetic neutral and doubly charged vacancies seems to preclude simple oxygen vacancies from being the mediator of ferromagnetism in $Zn_{1-x}Co_xO$. The mechanism of exchange coupling is discussed and compared to that proposed by Dietl *et al.*[65] The differences in the models for exchange coupling described here lie in the degree of localization of the magnetic state responsible for exchange coupling (determined by the acceptor binding energies) and positions of their centroids (on the transition metal for the model of Dietl *et al.* or on the N_O or $V_O{}^+$ defect).

ACKNOWLEDGMENTS

This work was supported by the Irish Higher Education Authority under the PRTLI-IITAC2 program. The author wishes to acknowledge discussions with J. M. D. Coey, M. Venkatesan, D. C. Look, D. R. Gamelin, S. Krishnamurthy, and C. MacGuinness and the hospitality of R. J. Bartlett at the University of Florida.

APPENDIX: STRUCTURE OPTIMIZATION

Minimization of the total energy of the Co_{Zn} defect, by varying positions of ions which lie within 3.5 Å of the Co^{2+} ion, results in changes in Co-O bond lengths to 1.98 Å parallel to the *c* axis and 1.97 Å in the *ab* plane. This corresponds to an expansion of the Zn-O bond parallel to the *c* axis by 0.03 Å and a slight contraction of bonds nearly in the *ab* plane by 0.01 Å.

When positions of ions within 3.5 Å of the V_O vacancy site were varied to minimize the total energy, the Zn ions immediately neighboring the vacancy site relaxed inwards by 0.25 Å for the Zn-O bond parallel to the *c* axis and by 0.14 Å for Zn-O bonds nearly parallel to the *ab* plane so that the nearest Zn-Zn distances for these ions were reduced from 3.21 and 3.25 Å to 2.89 and 2.97 Å, respectively. These relaxed bond distances are several percent shorter than those obtained previously in a DFT pseudopotential calculation which used a plane-wave basis set[51] but are close to the distances found for the neutral oxygen vacancy in ZnO in a more recent plane wave DFT study.[35]

O ions around the Zn vacancy relax outwards by 0.14 Å for the Zn-O bond parallel to the *c* axis and by 0.16 Å for the remaining three O ions nearest to the vacancy site.

The 12 Zn and O ions closest to the interstitial Zn, as well as the interstitial itself, were relaxed for the neutral Zn_i vacancy calculations described above. The optimized Zn_i-Zn distances were 2.36 and 2.47 Å and the Zn_i-O distances were 2.06 and 2.68 Å.

Ionic radii of O and N ions are similar, and so only a small distortion of the ZnO lattice is found when the structure of the N_O defect is allowed to relax. The Zn-N bond lengths parallel to the *c* axis and nearly parallel to the *ab* plane are 1.94(6) Å and 1.97(6) Å, respectively, which compares to Zn-O bond lengths of 1.952 and 1.985 Å in bulk ZnO.

*Permanent address: School of Physics, University of Dublin, Trinity College, Dublin 2, Ireland.

[1] K. Ueda, H. Tabata, and T. Kawai, Appl. Phys. Lett. **79**, 988 (2001).
[2] J. Kim, H. Kim, D. Kim, Y. Ihm, and W. Choo, J. Appl. Phys. **92**, 6066 (2002).
[3] H. Lee, S. Jeong, C. Cho, and C. Park, Appl. Phys. Lett. **81**, 4020 (2002).
[4] M. Venkatesan, C. B. Fitzgerald, J. G. Lunney, and J. M. D. Coey, Phys. Rev. Lett. **93**, 177206 (2004).
[5] D. A. Schwartz and D. R. Gamelin, Adv. Mater. (Weinheim, Ger.) **16**, 2115 (2004).
[6] K. R. Kittilstved, N. S. Norberg, and D. R. Gamelin, Phys. Rev. Lett. **94**, 147209 (2005).
[7] A. Hausmann and H. Huppertz, J. Phys. Chem. Solids **29**, 1369 (1968).
[8] N. Jedrecy, H. J. von Bardeleben, Y. Zheng, and J. L. Cantin, Phys. Rev. B **69**, 041308(R) (2004).
[9] I. Ozerov, F. Chabre, and W. Marine, Mater. Sci. Eng., C **25**, 614 (2005).
[10] K. R. Kittilstved and D. R. Gamelin, J. Am. Chem. Soc. **127**, 5292 (2005).
[11] J. F. Chang, W. C. Lin, and M. H. Hon, Appl. Surf. Sci. **183**, 18 (2001).
[12] A. C. Tuan *et al.*, Phys. Rev. B **70**, 054424 (2004).
[13] A. D. Becke, J. Chem. Phys. **98**, 5648 (1993).
[14] P. J. Stephens, F. J. Devlin, C. F. Chabalowski, and M. J. Frisch, J. Phys. Chem. **98**, 11623 (1994).
[15] A. S. Risbud, N. A. Spaldin, Z. Q. Chen, S. Stemmer, and R. Seshadri, Phys. Rev. B **68**, 205202 (2003).
[16] N. A. Spaldin, Phys. Rev. B **69**, 125201 (2004).
[17] E. C. Lee and K. J. Chang, Phys. Rev. B **69**, 085205 (2004).
[18] L. Petit, T. C. Schulthess, A. Svane, Z. Szotek, W. M. Temmermann, and A. Janotti, Phys. Rev. B **73**, 045107 (2006).

[19] M. H. F. Sluiter, Y. Kawazoe, P. Sharma, A. Inoue, A. R. Raju, C. Rout, and U. V. Waghmare, Phys. Rev. Lett. **94**, 187204 (2005).
[20] R. L. Martin and F. Illas, Phys. Rev. Lett. **79**, 1539 (1997).
[21] F. Cora, M. Alfredsson, G. Mallia, D. Middlemiss, W. C. Mackrodt, R. Dovesi, and R. Orlando, Struct. Bonding (Berlin) **113**, 171 (2004).
[22] X. Feng, J. Phys.: Condens. Matter **16**, 4251 (2004).
[23] K. A. Müller and J. Schneider, Phys. Lett. **4**, 288 (1963).
[24] R. S. Anderson, Phys. Rev. **164**, 398 (1967).
[25] A. Hausmann, Phys. Status Solidi **31**, K131 (1969).
[26] P. Koidl, Phys. Rev. B **15**, 2493 (1977).
[27] D. C. Reynolds, D. C. Look, B. Jogai, J. E. van Nostrand, R. Jones, and J. Jenny, Solid State Commun. **106**, 701 (1998).
[28] W. E. Carlos, E. R. Glaser, and D. C. Look, Physica B **308-310**, 976 (2001).
[29] F. Leiter, H. Zhou, F. Henecker, A. Hofstaetter, D. M. Hoffmann, and B. K. Meyer, Physica B **308-310**, 908 (2001).
[30] Y. V. Gorelkinskii and G. D. Watkins, Phys. Rev. B **69**, 115212 (2004).
[31] L. S. Vlasenko and G. D. Watkins, Phys. Rev. B **71**, 125210 (2005).
[32] F. Tuomisto, K. Saarinen, D. C. Look, and G. C. Farlow, Phys. Rev. B **72**, 085206 (2005).
[33] D. C. Look, J. W. Hemsky, and J. R. Sizelove, Phys. Rev. Lett. **82**, 2552 (1999).
[34] F. Tuomisto, V. Ranki, K. Saarinen, and D. C. Look, Phys. Rev. Lett. **91**, 205502 (2003).
[35] P. Erhart, A. Klein, and K. Albe, Phys. Rev. B **72**, 085213 (2005).
[36] S. B. Zhang, S. H. Wei, and A. Zunger, Phys. Rev. B **63**, 075205 (2001).
[37] C. H. Park, S. B. Zhang, and S. H. Wei, Phys. Rev. B **66**, 073202 (2002).
[38] M. Diaconu, H. Schmidt, A. Pöppl, R. Böttcher, J. Hoentsch, A. Klunker, D. Spemann, H. Hochmuth, M. Lorenz, and M. Grundmann, Phys. Rev. B **72**, 085214 (2005).
[39] M. Kobayashi *et al.*, Phys. Rev. B **72**, 201201 (2005).
[40] V. R. Saunders *et al.*, Crystal03 User's Manual, University of Torino, Torino, 2003 (www.crystal.unito.it).
[41] *Numerical Data and Functional Relationships in Science and Technology*, Landolt-Börnstein, New Series, Group III, Vols. 17a and 22a, edited by K. H. Hellwege and O. Madelung (Springer, New York, 1982).
[42] C. Van de Walle and J. Neugebauer, J. Appl. Phys. **95**, 3851 (2004).
[43] J. E. Jaffe and A. C. Hess, Phys. Rev. B **48**, 7903 (1993).
[44] M. D. Towler, N. L. Allan, N. M. Harrison, V. R. Saunders, W. C. Mackrodt, and E. Aprà, Phys. Rev. B **50**, 5041 (1994).
[45] R. Dovesi, F. Freyria-Fava, C. Roetti, and V. R. Saunders, Faraday Discuss. **106**, 173 (1997).
[46] R. Pandey, J. E. Jaffe, and N. M. Harrison, J. Phys. Chem. Solids **55**, 1357 (1994).
[47] A. Kokalj, Comput. Mater. Sci. **28**, 155 (2003).
[48] Code available from http://www.xcrysden.org
[49] *Data in Science and Technology; Semiconductors Other than Group IV Elements and III-V Compounds*, edited by O. Madelung (Springer-Verlag, Berlin, 1992), pp. 26–27.
[50] P. Schröer, P. Krüger, and J. Pollmann, Phys. Rev. B **47**, 6971 (1993).
[51] A. F. Kohan, G. Ceder, D. Morgan, and Chris G. Van de Walle, Phys. Rev. B **61**, 15019 (2000).
[52] S. C. Wi *et al.*, Appl. Phys. Lett. **84**, 4233 (2004).
[53] L. Hedin, Phys. Rev. **139**, A796 (1965).
[54] M. S. Hybertsen and S. G. Louie, Phys. Rev. Lett. **55**, 1418 (1985).
[55] A. Janotti and C. G. van de Walle, Appl. Phys. Lett. **87**, 122102 (2005).
[56] E.-C. Lee, Y.-S. Kim, Y.-G. Jin, and K. J. Chang, Phys. Rev. B **64**, 085120 (2001).
[57] D. C. Look, G. C. Farlow, P. Reunchan, S. Limpijumnong, S. B. Zhang, and K. Nordlund, Phys. Rev. Lett. **95**, 225502 (2005).
[58] D. C. Look and B. Clafin, Phys. Status Solidi B **241**, 624 (2004).
[59] K. Sato and H. Katayama-Yoshida, Semicond. Sci. Technol. **17**, 367 (2002).
[60] C. V. de Walle, Physica B **308-310**, 899 (2001).
[61] V. Gavryushin, G. Raciukaitis, D. Juodzbalis, A. Kazlauskas, and V. Kubertavicius, J. Cryst. Growth **138**, 924 (1994).
[62] P. Wagner and R. Helbig, J. Phys. Chem. Solids **35**, 327 (1974).
[63] D. C. Look, D. Reynolds, J. R. Sizelove, R. Jones, C. Litton, G. Cantwell, and W. Harsch, Solid State Commun. **105**, 399 (1998).
[64] D. C. Look, D. C. Reynolds, C. W. Litton, R. L. Jones, D. B. Eason, and G. Cantwell, Appl. Phys. Lett. **81**, 1830 (2002).
[65] T. Dietl, H. Ohno, F. Matsukura, J. Cibert, and D. Ferrand, Science **287**, 1019 (2000).
[66] S. Krishnamurthy and C. MacGuinness (private communication).
[67] C. H. Park and D. J. Chadi, Phys. Rev. Lett. **94**, 127204 (2005).
[68] J. M. D. Coey, M. Venkatesan, and C. B. Fitzgerald, Nat. Mater. **4**, 173 (2005).
[69] K. R. Kittilstved, W. K. Liu, and D. R. Gamelin, Nat. Mater. **5**, 291 (2006).